Supporting Information

Reliable sizing-up of 3D curved circular microchannel reactor for continuous flow synthesis of zidovudine intermediate

Haohui Yan,[a] Yan Chen,[a] Peiwen Liu,[a] Weiping Zhu*[a b] and Fang Zhao*[c]

[a] State Key Laboratory of Bioreactor Engineering, Shanghai Key Laboratory of Chemical Biology, School of Pharmacy, East China University of Science and Technology, Shanghai 200237, China.

[b] Engineering Research Center of Pharmaceutical Process Chemistry, Ministry of Education, School of Pharmacy, East China University of Science and Technology, Shanghai 200237, China.

[c] State Key Laboratory of Chemical Engineering, School of Chemical Engineering, East China University of Science and Technology, Shanghai 200237, China.

Corresponding Author

*To whom correspondence should be addressed. E-mail: fzhao1@ecust.edu.cn (Fang Zhao), wpzhu@ecust.edu.cn (Weiping Zhu)

Table of Content

1. Fitting of energy dissipation coefficient S3

2. Calculation for the values of α and β in the laminar flow and highly turbulent flow S5

3. HPLC analysis method S6

4. Fabrication of 3D-CCMRs S7

5. Assumptions of the mass transfer coefficient calculation formula S8

6. Possible reaction mechanism S8

7. The location of the cross-section in Fig. 8 of the manuscript S9

8. The cross-sections selected for the calculation of mixing index S10

9. Typical grid cross-section in ICEM S11

10. Measurement of actual energy consumption S11

1. Fitting of energy dissipation coefficient

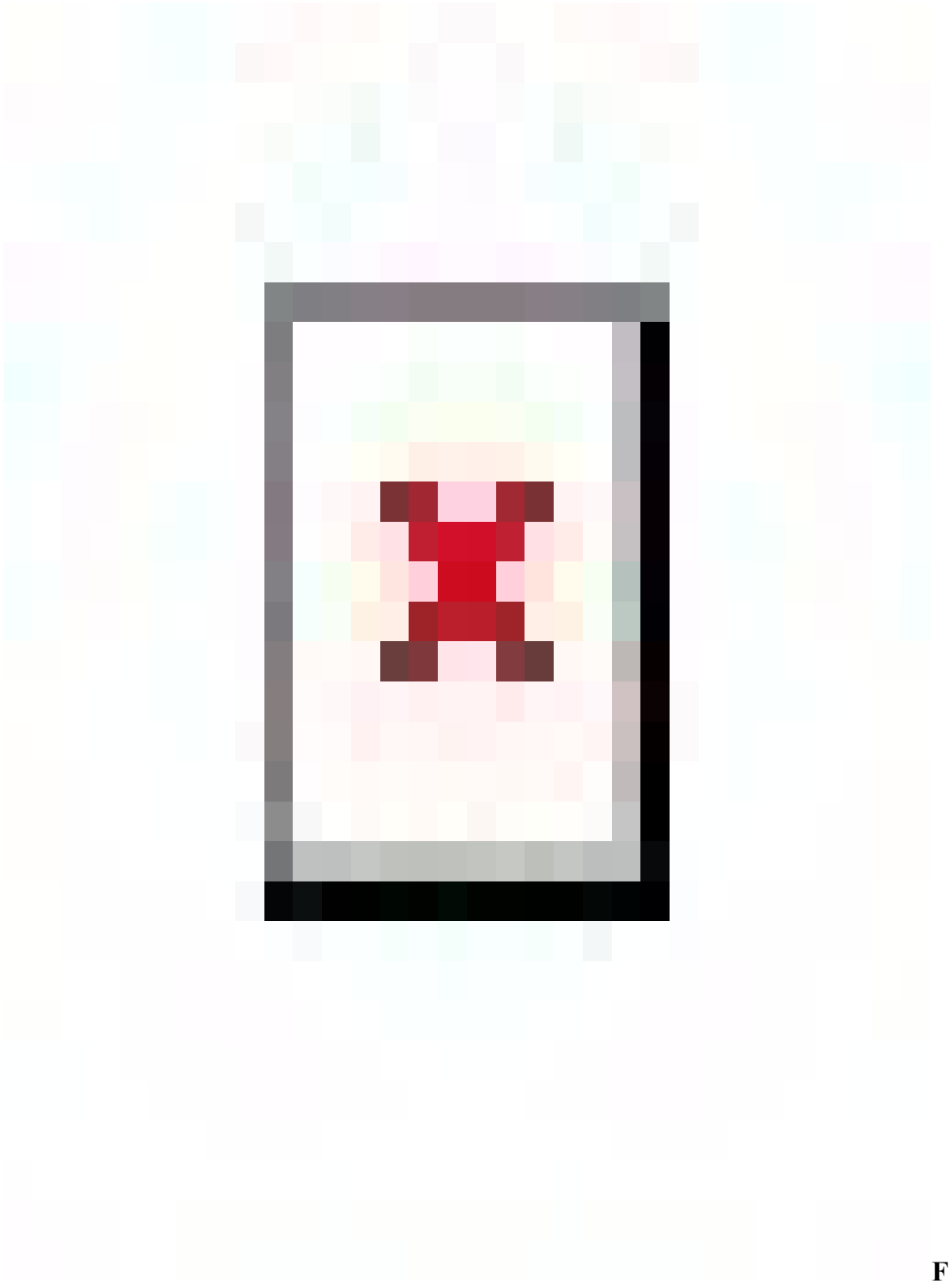

Fig. S1 The plots and linear fittings of lgε ~ lg$F$ for different channel diameters. The dashed lines represent the linear fitting lines. (a) D = 1 mm. (b) D = 1.2 mm. (c) D = 1.5 mm. (d) D = 1.8 mm. (e) D = 2 mm.

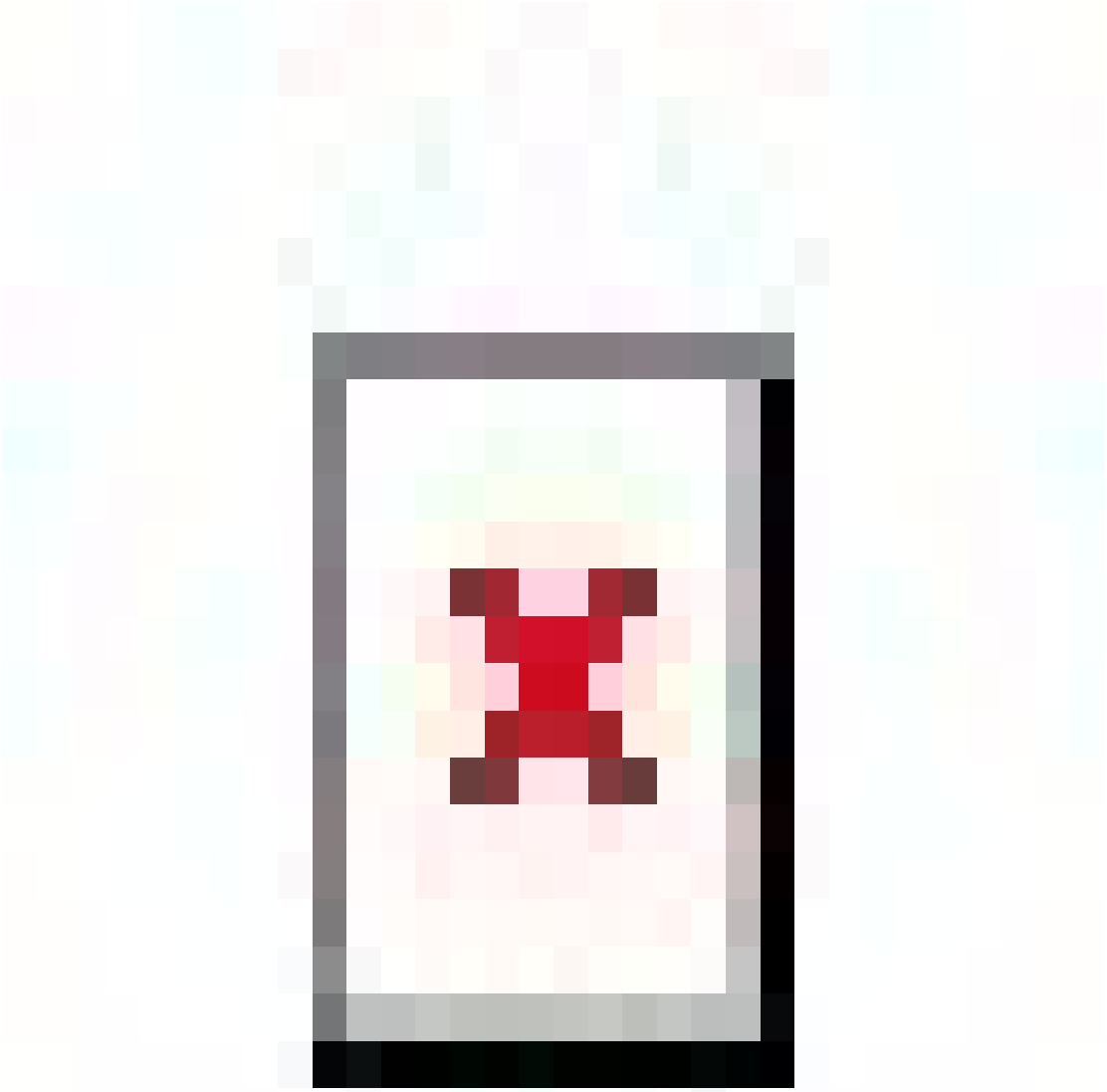

Fig. S2 The plots and linear fittings of lgε ~ lg$D$ for different flow rates. The dashed lines represent the linear fitting lines. (a) F = 1 mL·min^{-1}. (b) F = 2 mL·min^{-1}. (c) F = 4 mL·min^{-1}. (d) F = 8 mL·min^{-1}. (e) F = 15 mL·min^{-1}.

2. Calculation for the values of α and β in the laminar flow and highly turbulent flow

i)

Under laminar flow condition, according to the Hagen–Poiseuille equation, the pressure drop can be expressed by:

$$\Delta P = \frac{32\mu L u}{D^2}$$

where L is the channel length, and μ is the dynamic viscosity.

The flow velocity u can be expressed by the flow rate F:

$$u = \frac{F}{\frac{\pi}{4}D^2}$$

Then the energy dissipation rate is

$$\varepsilon = \frac{\Delta P \cdot F}{\rho \cdot V} = \frac{\frac{32\mu L}{D^2}\left(\frac{F}{\frac{\pi}{4}D^2}\right) \cdot F}{\rho \cdot \frac{\pi}{4}D^2 \cdot L} = \frac{512\mu}{\pi^2 \rho} \cdot \frac{F^2}{D^6} \propto \frac{F^2}{D^6}$$

where V is the channel volume, and ρ is the fluid density.

Therefore, the values of α and β are 2 and 6 for laminar flow, respectively.

ii)

For turbulent flow, the pressure drop can be given by:

$$\Delta P = \lambda \frac{\rho L}{D} \cdot \frac{u^2}{2}$$

where λ is the friction coefficient and can be regarded as a constant in a given channel

for highly turbulent flow in the region of the quadratic resistance law.

Then the energy dissipation rate is

$$\varepsilon = \frac{\Delta P \cdot F}{\rho \cdot V} = \frac{\lambda \frac{\rho L}{2D} \cdot \left(\frac{F}{\frac{\pi}{4} D^2} \right)^2 \cdot F}{\rho \cdot \frac{\pi}{4} D^2 \cdot L} = \frac{32\lambda}{\pi^3} \cdot \frac{F^3}{D^8} \propto \frac{F^3}{D^8}$$

Therefore, the values of α and β are 3 and 7 for for highly turbulent flow, respectively.

3. HPLC analysis method

Instrument: Shimadzu 2014C

Column: XBridge BEH Phenyl-Hexyl Colum, 3.5 μm, 4.6 mm×150 mm (Waters Technologies Shanghai Limited)

Mobile phase: water (Ultrapure water), methanol (HPLC grade)

Gradient elution method: 0-5 min, 5% methanol; 5-15 min, methanol concentration uniformly rises to 90%; 15-28 min 90% methanol; 28-33 min, methanol concentration uniformly decreases to 5%, 33-36 min 5% methanol

Total flow rate: 1.0 mL·min^{-1}

Injection volume: 2 μL

Column temperature: 35^{o}C

Detection wavelength: 254 nm.

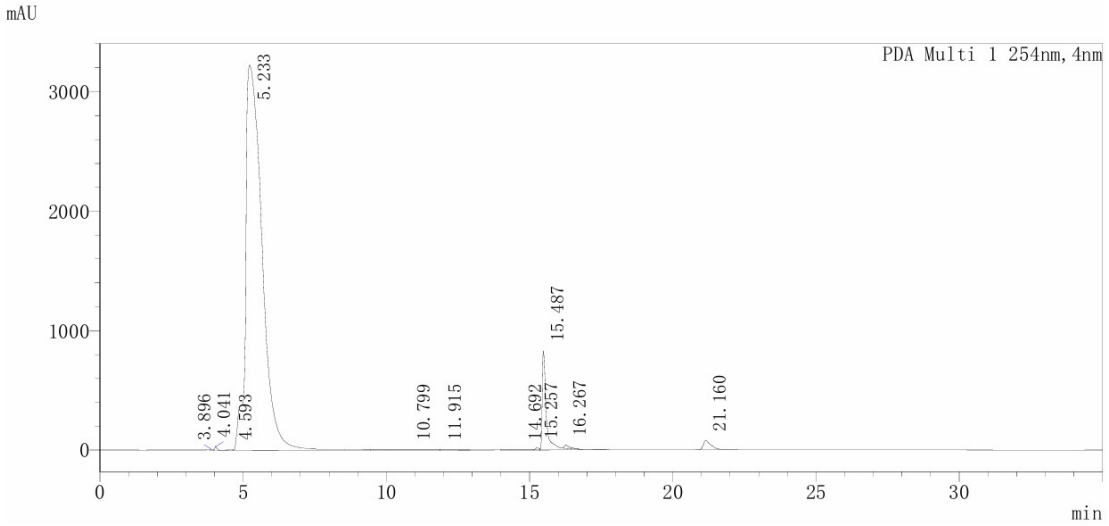

Fig. S3 Typical HPLC chromatogram for the continuous flow synthesis of AZT-A. Thymidine-, 4.041 min; pyridine at 5.233 min; AZT-A, 15.487 min.

4. Fabrication of 3D-CCMRs

The two 3D-CCMRs in this work were both manufactured by internal graving via the femtosecond laser technology. First, a borosilicate glass plate was mounted on a 3D positioning stage controlled by a motion controller (A3200, Aerotech). A femtosecond laser source (Pharos 20 W, Light Conversion Ltd) with a central wavelength of 1030 nm, a pulse width of 270 fs, and a repetition rate of 200 kHz was used for laser modification of the glass, and the glass plate was irradiated by the focused laser beam using a 5×objective lens (Mitutoyo, Japan) with a numerical aperture of 0.14. Next, the glass was immersed in an ultrasonic bath of KOH aqueous solution to selectively remove the laser-modified area. Finally, the glass was cleaned with isopropyl alcohol and deionized water, and then mildly annealed.

5. Assumptions of the mass transfer coefficient calculation formula

According to the literature (DOI:10.1016/j.cclet.2023.108833), the equation to calculate $k_L a$ (eqn (8) in the manuscript) were derived based the following assumptions: *i*) the mass transfer resistance in the gas phase and that for CO_2 dissolution at the gas-liquid interface were both negligible as compared to that in the liquid phase, so that the interfacial concentration of CO_2 on the liquid side was the equilibrium liquid concentration corresponding to the CO_2 pressure in the gas phase, i.e., $C^*_{CO_2}$; *ii*) equilibrium of CO_2 dissolution in the water followed the Henry's law; *iii*) the liquid buck concentration of CO_2 could be regarded as zero due to very low absorption amount of CO_2.

6. Possible reaction mechanism

Due to steric hindrance, triphenyl chloromethane is often used to regionally selectively protect the primary hydroxyl group. The synthetic mechanism of AZR-A that we hypothesized is shown in Figure S3. In the alkaline condition of pyridine as solvent, the N on pyridine forms a nitrogen hydrogen bond with the H on the primary hydroxyl of thymidine, while the chlorine on triphenylchlormethane is removed to form a carbanion, which is then attacked by a lone pair of electrons on the oxygen on the primary hydroxyl of thymidine. At the same time, the hydrogen oxygen bond on the primary hydroxyl of thymidine is broken to form AZT-A and Pyridinium.

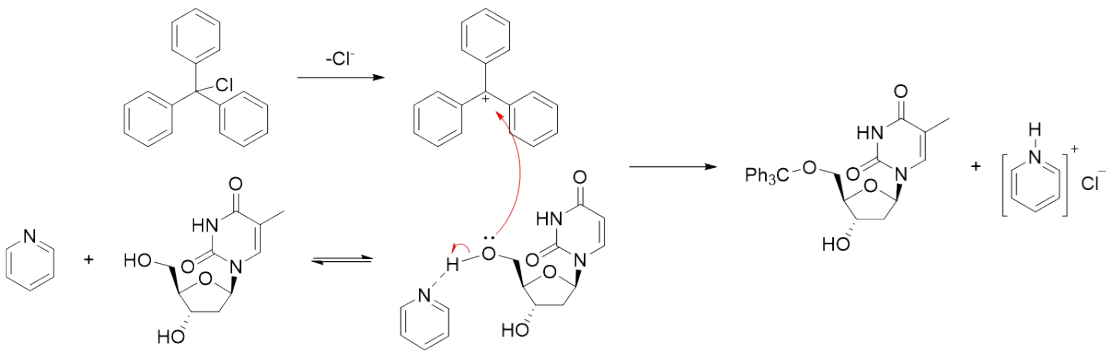

Fig. S4 Plausible mechanism for the synthesis of Zidovudine intermediate AZT-A

7. The location of the cross-section in Fig. 8 of the manuscript

The positions of the cross-sections in Fig. 8 are shown below. When the flow velocity u = 0.01 m·s^{-1}, the two positions in the two different microchannels (n = 1 and 2) both corresponded to a residence time t_{RT} = 34 ms. As shown in Fig. S4, in the n = 1 microchannel, the cross section is located at the eighth bend of the first unit, and in the n = 2 microchannel, the cross section is located at the sixth bend of the first unit.

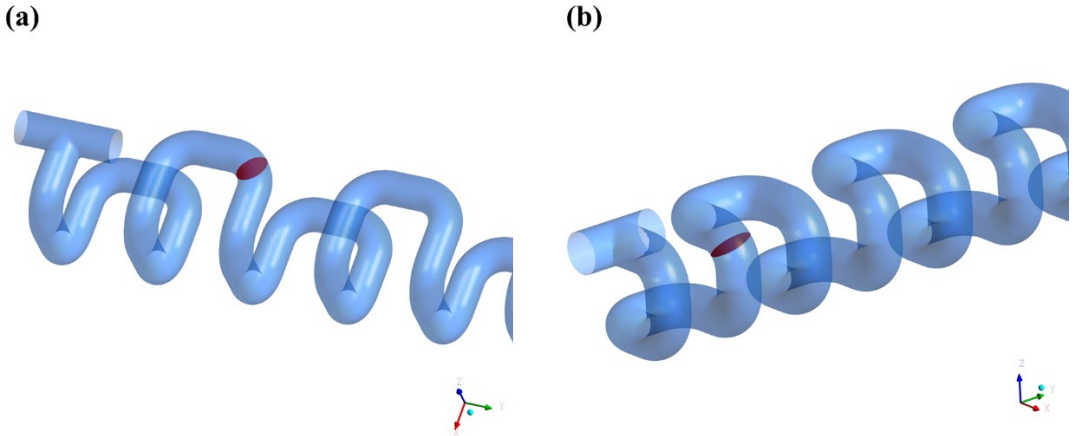

Fig. S5 The positions of the cross-sections selected in the two microchannels at different n for a velocity u = 0.01 m • s^{-1} and residence time t_{RT} = 34 ms. (a) n = 1. (b) n = 2.

8. The cross-sections selected for the calculation of mixing index

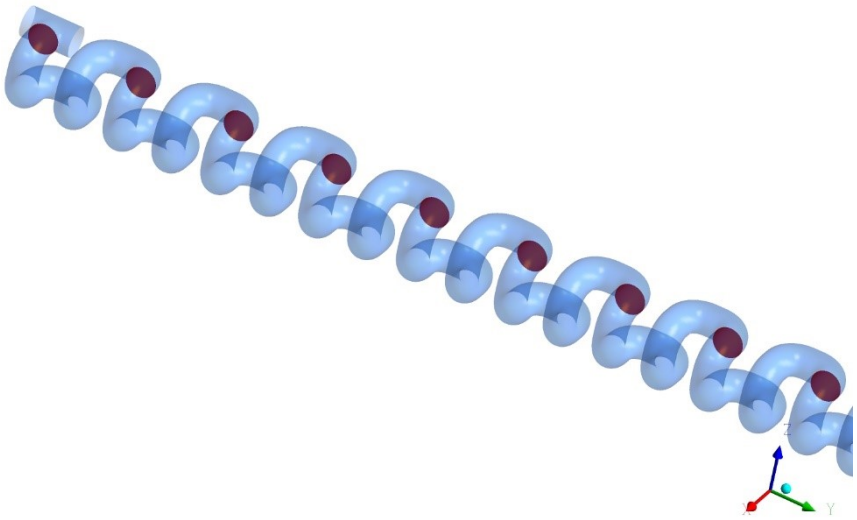

Fig. S6 The cross-sections selected (marked as red) for calculating the mixing index: the cross-section at the beginning of the first microchannel unit, and those at the end of each microchannels unit (1st, 2nd, 3rd, …). This figure shows the microchannel at n = 2 mm.

9. Typical grid cross-section in ICEM

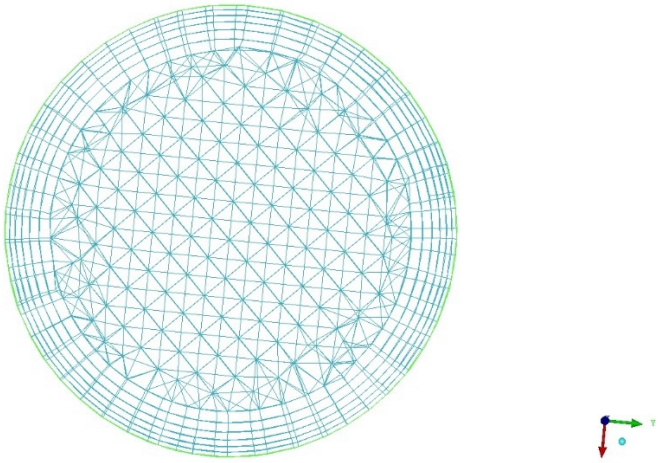

Fig. S7 Typical mesh cross-section generated by ICEM for 3D curved circular microchannel.

10. Measurement of actual energy consumption

We measured the pressure drops of 3D-CCMR-1 and 3D-CCMR-2 at different flow rates, and calculated their energy dissipation rates ε. As shown in Fig. S8, the experimentally determined $\lg\varepsilon$ had a good linear relationship with $\lg F$ in both 3D-CCMR-1 and 3D-CCMR-2, with slopes of 2.60 and 2.75, respectively. According to Fig. 9 of the manuscript, the slope of the linear fitting line of $\lg\varepsilon \sim \lg F$ for the 3D curved circular microchannel determined by CFD simulation was 2.35, which was close to the experimental results (the small deviation was possibly ascribed to the inaccuracy in the flow rate of the pump used in the experiment).

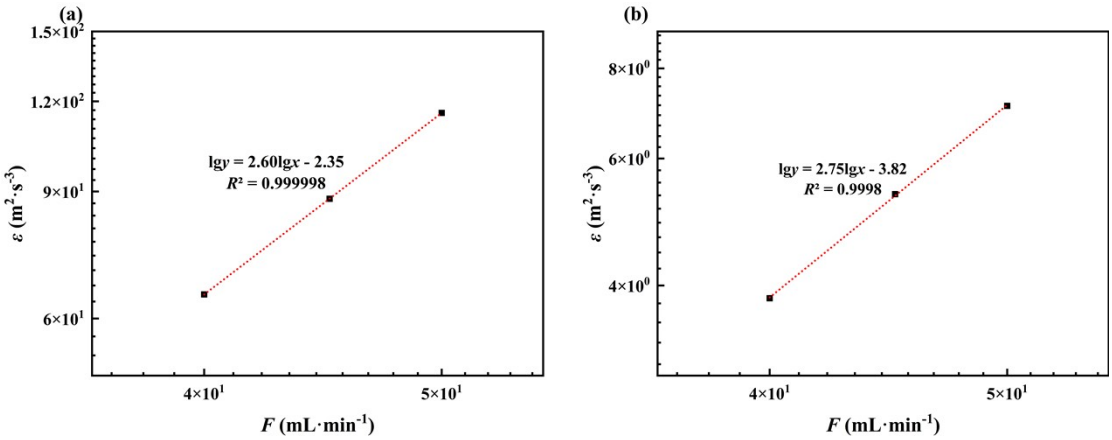

Fig. S8 The change of the energy dissipation rate ε measured by experiment with the flow rate F in two reactors. (a) 3D-CCMR-1. (b) 3D-CCMR-2.